Testing Charmonium Production Mechanism via Polarized J/ψ Pair Production at the LHC

Cong-Feng Qiao[1,2], Li-Ping Sun[1], Peng Sun[1]

[1] *College of Physical Sciences, Graduate University of Chinese Academy of Sciences YuQuan Road 19A, Beijing 100049, China and*

[2] *Theoretical Physics Center for Science Facilities (TPCSF), CAS YuQuan Road 19B, Beijing 100049, China*

Abstract

At present the color-octet mechanism is still an important and debatable part in the non-relativistic QCD(NRQCD). We find in this work that the polarized double charmonium production at the LHC may pose a stringent test on the charmonium production mechanism. Result shows that the transverse momentum(p_T) scaling behaviors of double J/ψ differential cross sections in color-singlet and -octet production mechanisms deviate distinctively from each other while p_T is larger than 7 GeV. In color-octet mechanism, the two J/ψs in one pair are mostly transversely polarized when $p_T \gg 2m_c$, as expected from the fragmentation limit point of view. In color-singlet mechanism, there is about one half of the charmonium pairs with at least one J/ψ being longitudinally polarized at moderate transverse momentum. The energy dependence of the polarized J/ψ pair production is found to be weak, and this process is found to be experimentally attainable in the early phase of the LHC operation.

PACS numbers: 12.38.Bx, 13.85.Fb, 14.40.Lb.

I. INTRODUCTION

NRQCD[1] has now become a basic theory to parameterize non-perturbative contributions in heavy quarkonium production and decays by color-singlet(CS) and color-octet(CO) matrix elements. It defines the "velocity scaling rules" to order various matrix elements by v, the relative velocity of heavy quarks in the rest frame of heavy quarkonium. Although NRQCD has already achieved a lot in the study of heavy quarkonium physics, there are still some unsettled issues remaining, especially, in aspect of production mechanism [2], for instance, the role of color-octet in charmonium production.

The color-octet scheme is a central essence of NRQCD, which supplies a way to partly understand the prompt J/ψ and ψ' surplus production at the Fermilab Tevatron [3], and supplies a consistent differential cross section spectrum, versus the transverse momentum p_T, with experimental results [4]. However, there are still something unclear in this scheme, which ask for further effort. In electron-positron collision, the former crises in J/ψ exclusive [5–7] and inclusive production [8, 9] are somehow going to an end with the advent of the next-to-leading order(NLO) QCD [10, 11] and relativistic correction results [12]. In charmonium photoproduction, the recent NLO QCD calculation tells that to reproduce the full HERA experimental results, the color-singlet contribution alone seems not enough [13]. In charmonium hadroproduction, recent computations of NLO QCD corrections [14] significantly enhance the J/ψ color-singlet yield in large transverse momentum region and alter its polarization prediction in LO calculation. Hence, the NLO J/ψ hadroproduction result in CS scheme greatly minimize the contribution through color-octet mechanism, which in some sense agrees with the hypotheses given in Ref.[15]. For more detailed discussion on these issues, readers can refer to recent review articles, e.g., [16–18].

To further investigate charmonium production mechanism keeps on being an urgent and important task in the study of quarkonium physics. The running of the LHC supplies a great opportunity to this aim. With a luminosity of about $10^{32} \sim 10^{34} cm^{-2} s^{-1}$ and center of mass energy $7 \sim 14$ TeV, LHC will produce copious data of charmonium inclusive and exclusive production, which can in principle answer the question: to what extent the color-octet mechanism plays a role in ψ production? As noted by Cho and Wise that the direct ψ production via color-octet mechanism should be mostly transversely polarized at leading

order in α_s, which may stand as a unique test to the quarkonium production mechanism [19]. In this work, we consider the process of polarized J/ψ pair production at LHC, and suggest to test the charmonium production mechanism through it. The same process but in unpolarized case was proposed and calculated by Barger *et al.* [20] and Qiao [21] once for Tevatron experiment.

The paper is organized as follows: In section II, we set up the formalism for the computation of polarized ψ hadroproduction, in both color-singlet and -octet schemes. In section III, the numerical results for the LHC first-year and later runs are provided. The section IV is remained for a brief summary and conclusions. For the convenience of readers, the relevant analytic expressions are given in the Appendix.

II. FORMALISM

A. Color-Singlet Scheme

In color-singlet model, the partonic subprocesses start at order α_s^4, which include $g+g \to J/\psi + J/\psi$ and $q+\bar{q} \to J/\psi + J/\psi$. Intuitively, the latter, the quark-antiquark annihilation process, is possibly negligible in comparison with the former since the LHC is a proton-proton collision machine. To confirm this point, the quark-antiquark process is also evaluated in this work and the numerical result is given in Table I. Hence, in the following analysis we will mainly focus on the gluon-gluon process as shown in Figure 1, and the analytic results

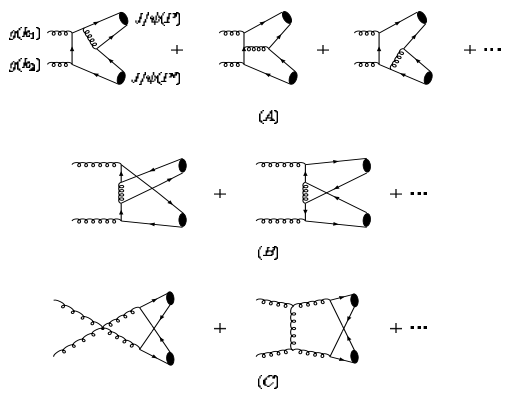

FIG. 1: Typical Feynman diagrams of J/ψ pair production in $p\,p$ collision at leading order in color-singlet scheme.

of it are presented in the Appendix.

For $J/\psi(^3S_1)$ color-singlet hadronization, we employ the following commonly used projection operator

$$v(p_{\bar{c}})\,\overline{u}(p_c) \;\longrightarrow\; \frac{1}{2\sqrt{2}}\,\not{\epsilon}^*_{J/\psi}\,(\not{P}+2m_c)\;\times\left(\frac{1}{\sqrt{m_c}}\psi_{J/\psi}(0)\right)\otimes\left(\frac{\mathbf{1}_c}{\sqrt{N_c}}\right)\,, \tag{1}$$

where $\epsilon^{\mu}_{J/\psi}$ is the J/ψ polarization vector with $P\cdot\varepsilon=0$, $\mathbf{1}_c$ stands for the unit color matrix, and $N_c=3$. The nonperturbative parameter, $\psi_{J/\psi}(0)$, is the Schrödinger wave function of c and $\bar{c}$ system at the origin for J/ψ, and $|\psi_{J/\psi}(0)|=\sqrt{|R(0)|^2/4\pi}$ with $R(0)$ being the radial wave function at the origin. In our calculation, the non-relativistic relation $m_{J/\psi}=2m_c$ is adopted, and hereafter, for simplicity $m_{J/\psi}$ will be denoted by m.

The differential cross section for J/ψ pair hadroproduction reads as

$$\frac{d\sigma}{dp_T}(pp\to 2J/\psi+X)=\sum_{a,b}\int dy_1dy_2f_{a/p}(x_a)f_{b/p}(x_b)2p_Tx_ax_b\frac{d\hat{\sigma}}{dt}(a+b\to 2J/\psi)\,, \tag{2}$$

where $f_{a/p}$ and $f_{b/p}$ denote the parton densities; y_1, y_2 are the rapidity of the two produced J/ψs. The partonic scattering process, the gluon-gluon to polarized J/ψ pair $\frac{d\hat{\sigma}}{dt}$, can be calculated in the standard method. To manipulate the trace and matrix-element-square for those diagrams shown in Figure 1, the computer algebra system MATHEMATICA is employed with the help of the package FEYNCALC and FEYNARTS [22]. The lengthy expressions for different J/ψ pair polarizations are presented in the Appendix, for the convenience of independent comparison and physical simulation use. Summing over all polarizations, we find an agreement with the unpolarized cross section given in [21].

In experiment, the J/ψ polarizations can be determined via measuring the normalized angular distribution $I(\cos\theta)$ of $\mu^+\mu^-$ pair in J/ψ decays. The correlation of distribution with polarization reads [23, 24]

$$I(\cos\theta)=\frac{3}{2(\alpha+3)}(1+\alpha\,\cos^2\theta)\,. \tag{3}$$

Here, θ is the angle between the μ^+ direction in the J/ψ rest frame and the J/ψ direction in pp center-of-mass frame; α is a convenient measure of the polarization, which is defined as $\alpha=(\sigma_T-2\sigma_L)/(\sigma_T+2\sigma_L)$ where σ_T and σ_L are transverse and longitudinal components of the cross section, respectively. For detailed derivation of the relation between polarization measure α and decay distribution, see, e.g., the Appendix A of Ref. [24]. From the definition,

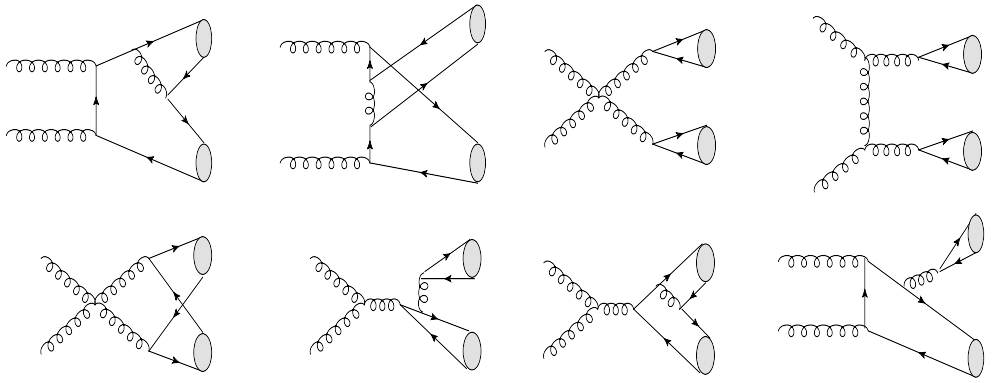

FIG. 2: Typical Feynman diagrams of J/ψ pair production in $p\,p$ collision at leading order in color-octet scheme.

obviously, $\alpha = 1$ corresponds to the transverse polarization, and $\alpha = -1$ to the longitudinal polarization.

B. Color-Octet Scheme

In NRQCD, the short-distant contribution can be expanded by v. Dynamical gluons enter into Fock state, and combine with heavy quark pair to form Color octet states. Therefore, wave functions of J/ψ is represented by

$$|J/\psi\rangle = O(1)|c\bar{c}[^3S_1^{(1)}]\rangle + O(v)|c\bar{c}[^3P_J^{(8)}]g\rangle + O(v^2)|c\bar{c}[^3S_1^{(1,8)}]gg\rangle + O(v^2)|c\bar{c}[^1S_0^{(8)}]g\rangle + ... \quad (4)$$

In the CO scheme, at the leading order of v, three different CO state components $|c\bar{c}[^3P_J^{(8)}]g\rangle$, $|c\bar{c}[^3S_1^{(1,8)}]gg\rangle$ and $|c\bar{c}[^1S_0^{(8)}]g\rangle$ may contribute to the double J/ψ production. In practice, for the sake of simplicity for further analysis, we classify the intermediate Fock states into two clusters: one contains $|c\bar{c}[^3S_1^{(1,8)}]gg\rangle$, the other includes $|c\bar{c}[^1S_0^{(8)}]g\rangle$ and $|c\bar{c}[^3P_J^{(8)}]g\rangle$. In this sense, the double J/ψ Fock states may have following different combinations:

$$\begin{aligned}
|J/\psi\rangle|J/\psi\rangle \;=\; & |c\bar{c}[^3S_1^{(1)}]\rangle|c\bar{c}[^3S_1^{(1)}]\rangle + \underbrace{|c\bar{c}[^3S_1^{(1)}]\rangle|c\bar{c}[^3S_1^{(8)}]gg\rangle}_{Part_1} \\
& + \underbrace{|c\bar{c}[^3S_1^{(1)}]\rangle(|c\bar{c}[^3P_J^{(8)}]g\rangle + |c\bar{c}[^1S_0^{(8)}]g\rangle)}_{Part_2} + \underbrace{|c\bar{c}[^3S_1^{(8)}]gg\rangle|c\bar{c}[^3S_1^{(8)}]gg\rangle}_{Part_3} \\
& + \underbrace{|c\bar{c}[^3S_1^{(8)}]gg\rangle(|c\bar{c}[^3P_J^{(8)}]g\rangle + |c\bar{c}[^1S_0^{(8)}]g\rangle)}_{Part_4}
\end{aligned}$$

$$+ \underbrace{(|c\bar{c}[^3P_J^{(8)}]g\rangle + |c\bar{c}[^1S_0^{(8)}]g\rangle)(|c\bar{c}[^3P_J^{(8)}]g\rangle + |c\bar{c}[^1S_0^{(8)}]g\rangle)}_{Part_5} \tag{5}$$

In (5) the leading one indicates the pure color-singlet state, which is discussed in the preceding subsection. The CO states involved components are then divided into five sectors. In small transverse momentum p_T region, where the NRQCD factorization theorem does not work well, the five CO state related processes would contribute less to the double charmonium production than from the pure CS process due to a suppression in matrix elements of v^4 or v^8. In large p_T region, however, the CO contribution, especially from $|c\bar{c}[^3S_1^{(8)}]gg\rangle$ may exceed what from the CS, because the relative smallness of CO matrix elements may be compensated by the enhancement of the large propagators in corresponding processes, which is similar to the case of inclusive ψ production in large transverse momentum region at the Fermilab Tevatron [4, 25]. In infinite transverse momentum limit, it is well-known that the process of gluon fragmenting into $|c\bar{c}[^3S_1^{(8)}]gg\rangle$ will dominate over others in ψ hadroproduction. Hence, one may still expect here that in the double J/ψ exclusive hadroproduction in the large transverse momentum region, the bi-gluon fragmentation would be the most important production mechanism. However, in moderate transverse momentum case as in LHC experiment, to minimize the uncertainties induced by the fragmentation mechanism we calculate the complete Feynman diagrams for CO processes instead of fragmentation simplification as shown in Figure 2.

For processes involving the CO components, that is $part_1$ to $part_5$ in (5), those contribute double J/ψ production via intermediate states $|c\bar{c}[^1S_0^{(8)}]g\rangle$ and $|c\bar{c}[^3P_J^{(8)}]g\rangle$ are obviously negligible in comparison with the CS process as shown in Figure 1. Moreover, the $part_4$ involved processes may contribute less than what from $part_1$ processes by v^4, an order. For $Part_1$ contribution, our explicit numerical calculation shows that it is smaller than what from the CS by about two orders of magnitude in all p_T region. In all, the meaningful CO contribution mainly comes from the $part_3$ involved processes, and which are what we are going to evaluate.

For the J/ψ intermediate Fock state $|c\bar{c}[^3S_1^{(8)}]gg\rangle$, the projection operator is

$$v(p_{\bar{c}})\,\overline{u}(p_c) \;\longrightarrow\; \frac{R_8(0)}{\sqrt{16\pi m_c}} T^a_{\bar{c}c}\, \not{\epsilon}^*_{J/\psi}\,(\not{P} + 2m_c)\,, \tag{6}$$

$$|R_8(0)|^2 = \frac{\pi}{6} < \mathcal{O}_8^{J/\psi}(^3S_1) > \;. \tag{7}$$

Except for the difference in CO and CS non-perturbative matrix element projections, the perturbative calculations of Feynman diagrams for both CS and CO are similar.

III. NUMERICAL RESULTS

In numerical calculation, we enforce the LHC experimental condition, the pseudorapidity cut $|\eta(J/\psi)| < 2.2$, on the produced charmonium pair. The cross sections and transverse momentum spectra are evaluated under three conditions: the first one with center-of-mass energy $\sqrt{S} = 7$ TeV, the second one with center-of-mass energy $\sqrt{S} = 10$ TeV, the third one with center-of-mass energy $\sqrt{S} = 14$ TeV, which correspond to the experimental situations of initial and following runs for hadron study at the LHC [26]. The planned collisions happen at the LHC with luminosity of $\sim 10^{32} cm^{-2} s^{-1}$ in first two cases, and $\sim 10^{33} cm^{-2} s^{-1}$ in the third situation. In one year running, $10^7 s$ effective time, the corresponding integrated luminosities are about $1(fb^{-1})$ and $10(fb^{-1})$, respectively. The input parameters take the values [25]

$$m_c = 1.5 \text{ GeV}, \ |\mathrm{R}(0)|^2 = 0.8 \text{ GeV}^3, \ < \mathcal{O}_8^{\mathrm{J}/\psi}(^3\mathrm{S}_1) >= 0.012 \text{ GeV}^3 \ . \tag{8}$$

The typical energy scale in partonic interaction is set to be at $m_T = \sqrt{m^2 + p_T^2}$, and hence the strong coupling is running with transverse momentum.

With the above formulas and inputs, one can readily obtain the polarized J/ψ pair production rate at the LHC. In our numerical calculation, the parton distribution functions(PDFs) of CTEQ5L[27] is used, and both renormalization scale in strong coupling α_s and factorization scale in PDFs are set to be m_T. The numerical results for integrated cross section $\sigma(p\ p \to J/\psi J/\psi)$ with different p_T lower bounds are presented in Table I for the CS production scheme, and Table II for the CO scheme, where the the branching fraction of $B(J/\psi \to \mu^+\mu^-) = 0.0597$ is taken into account.

The spectra of double-J/ψ exclusive production as function of transverse momentum p_T are illustrated in Figures 3 to 5. From these figures we see that the conventional CS production scheme dominates over the CO one in relatively low-p_T region, some $p_T < 7$ GeV.

TABLE I: The integrated cross sections of J/ψ pair production in color-singlet model under various transverse momentum lower cuts at the center-of-mass energy $\sqrt{S} = 7$ TeV, 10 TeV and 14 TeV. Here, $\perp\perp$ represents for the situation of both J/ψs being transversely polarized, $\|\|$ for both J/ψs being longitudinally polarized, $\|\perp$ for one J/ψ being longitudinally polarized and the other being transversely polarized. The tot_{gg} and $tot_{q\overline{q}}$ denote the polarization-summed cross sections of gluon-gluon fusion and quark-antiquark annihilation processes, respectively.

	7TeV					10TeV					14TeV				
$\sigma \setminus p_{Tcut}$	3 GeV	4 GeV	5 GeV	6 GeV	7 GeV	3 GeV	4 GeV	5 GeV	6 GeV	7 GeV	3 GeV	4 GeV	5 GeV	6 GeV	7 GeV
$\perp\perp$	2.07pb	0.61pb	0.20pb	0.070pb	0.027pb	2.84pb	0.85pb	0.29pb	0.10pb	0.039pb	3.81pb	1.16pb	0.38pb	0.14pb	0.055pb
$\|\|\|$	0.79pb	0.29pb	0.11pb	0.040pb	0.016pb	1.09pb	0.41pb	0.15pb	0.040pb	0.023pb	1.45pb	0.55pb	0.20pb	0.079pb	0.033pb
$\|\perp$	2.16pb	0.55pb	0.14pb	0.040pb	0.012pb	2.96pb	0.76pb	0.20pb	0.056pb	0.018pb	3.96pb	1.04pb	0.27pb	0.079pb	0.024pb
tot_{gg}	4.96pb	1.43pb	0.44pb	0.15pb	0.055pb	6.81pb	2.00pb	0.62pb	0.21pb	0.079pb	9.12pb	2.72pb	0.85pb	0.29pb	0.11pb
$tot_{q\overline{q}}$	0.040pb	0.013pb	4.27fb	1.57fb	0.64fb	0.047pb	0.015pb	5.12fb	1.90fb	0.77fb	0.056pb	0.017pb	6.12fb	2.28fb	0.93fb

TABLE II: The integrated cross sections of J/ψ pair production in color-octet model with various transverse momentum lower cuts at the center-of-mass energy $\sqrt{S} = 7$ TeV, 10 TeV and 14 TeV. Here, $\perp\perp_{88}$ represents for the situation of both J/ψs being transversely polarized, $\|\|_{88}$ for both J/ψs being longitudinally polarized, $\|\perp_{88}$ for one J/ψ being longitudinally polarized and the other being transversely polarized, and the tot_{88} means the polarization-summed CO cross section in gluon-gluon fusion. The tot_{18} in last row represents for the double J/ψ yields from CS + CO production scheme for reference.

	7TeV					10TeV					14TeV				
$\sigma \setminus p_{Tcut}$	3 GeV	4 GeV	5 GeV	6 GeV	7 GeV	3 GeV	4 GeV	5 GeV	6 GeV	7 GeV	3 GeV	4 GeV	5 GeV	6 GeV	7 GeV
$\perp\perp_{88}$	0.22pb	0.16pb	0.11pb	0.075pb	0.051pb	0.31pb	0.23pb	0.16pb	0.11pb	0.076pb	0.43pb	0.32pb	0.23pb	0.16pb	0.11pb
$\|\|\|_{88}$	1.33fb	0.43fb	0.14fb	0.051fb	0.020fb	1.84fb	0.60fb	0.20fb	0.073fb	0.029fb	2.46fb	0.81fb	0.28fb	0.10fb	0.040fb
$\|\perp_{88}$	0.025pb	0.013pb	6.95fb	3.62fb	1.93fb	0.035pb	0.019pb	9.95fb	5.25fb	2.84fb	0.047pb	0.026pb	0.014pb	7.36fb	4.02fb
tot_{88}	0.25pb	0.18pb	0.12pb	0.080pb	0.053pb	0.35pb	0.25pb	0.17pb	0.12pb	0.079pb	0.48pb	0.35pb	0.24pb	0.16pb	0.11pb
tot_{18}	0.15pb	0.047pb	0.015pb	5.14fb	1.95fb	0.21pb	0.065pb	0.021pb	7.37fb	2.83fb	0.29pb	0.089pb	0.029pb	0.010pb	3.97fb

IV. SUMMARY AND CONCLUSIONS

We have in this work evaluated the polarized J/ψ pair hadroproduction rate, directly and exclusively, at the LHC in color-singlet and -octet schemes. In color-octet scheme, Fock state $|c\bar{c}[^3S_1^{(8)}]gg\rangle|c\bar{c}[^3S_1^{(8)}]gg\rangle$ involved process dominates over others, and it yields mainly

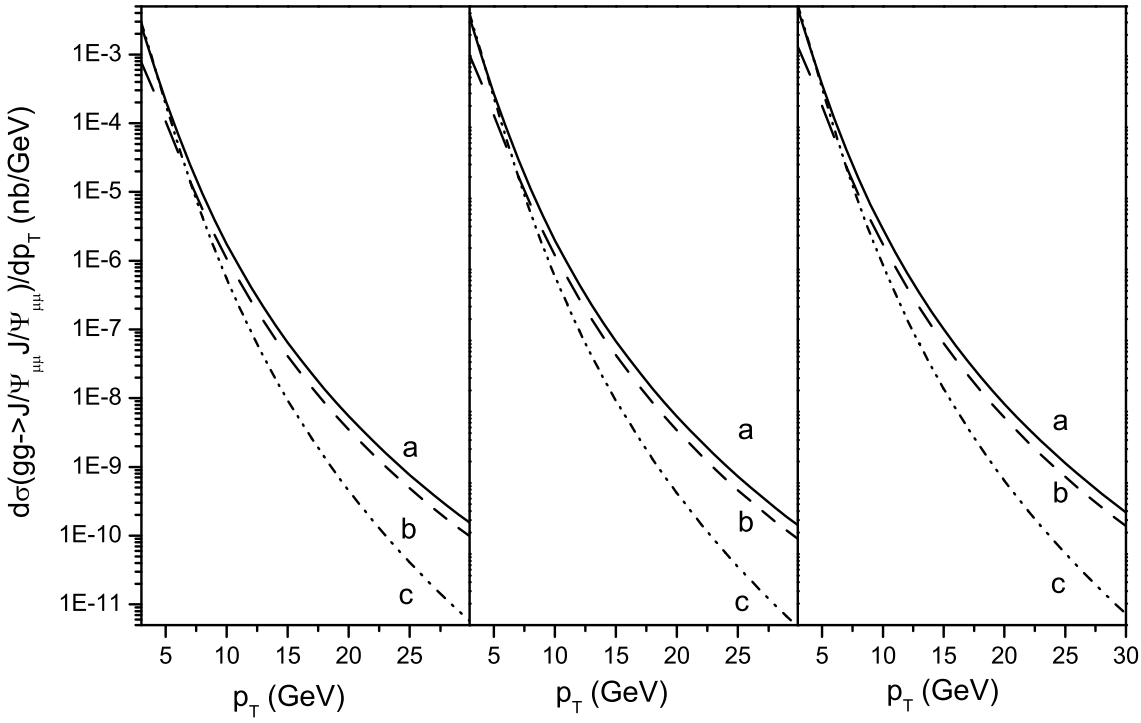

FIG. 3: The differential cross-section of J/ψ pair production versus p_T at the LHC in color-singlet scheme. Lines from top to bottom, i.e. a ,b and c, represent yields from color-singlet in $\perp\perp$, $\parallel\parallel$, and $\parallel\perp$ cases, respectively. The diagrams from left to right represent for cases of $\sqrt{S} = 7$ TeV, $\sqrt{S} = 10$ TeV, and $\sqrt{S} = 14$ TeV, respectively.

the transversely polarized J/ψs. Other CO related processes, either single or double CO processes, contribute significantly less than those from CS and $part_1$ involved processes in whole transverse momentum region, therefore can be neglected. Result shows that in low transverse momentum region the double J/ψ yields are governed by the CS process, while the CO process may dominate as $p_T > 7$ GeV. The indirect J/ψ production from the χ_{cJ} and ψ' feed down, according to the analysis of [20], may contribute about a factor of 2 to the transverse distribution spectrum of prompt J/ψ production, while these inclusive yields can be removed in experiment in principle and hence are not taken into account in our analysis.

The calculation performed in this work is at the leading order of strong coupling α_s. Due to the relatively high interaction scale in this process, higher order QCD corrections should

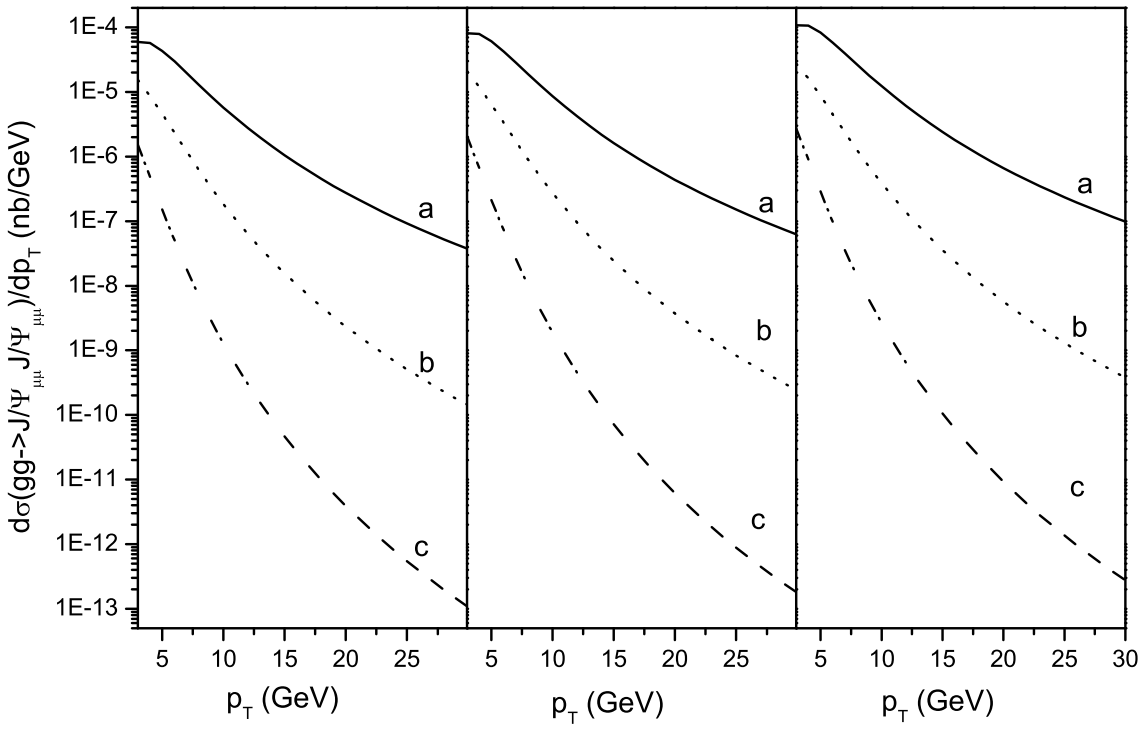

FIG. 4: The differential cross-section of J/ψ pair production versus p_T at the LHC in color-octet scheme. Lines from top to bottom, i.e. a ,b and c, represent yields from color-octet in $\perp\perp$, $\parallel\perp$, and $\parallel\parallel$ cases, respectively. The diagrams from left to right represent for cases of $\sqrt{S} = 7$ TeV, $\sqrt{S} = 10$ TeV, and $\sqrt{S} = 14$ TeV, respectively.

be small. The "smallness" here means that it may not be as big as NLO corrections to some inclusive charmonium production processes recently found. Nevertheless, this is just a naive speculation. For exclusive process, higher order corrections, the virtual corrections, do not change the relative polarization ratio, while is different from NLO correction to the inclusive process where the hard real correction may alter the final state polarization significantly. Though higher order relativistic correction is generally large in charmoniun system, while for J/ψ pair production it will be doubly suppressed. It is worthy of mentioning that in order to keep the exclusivity of double J/ψ production and reduce the final state interaction effects, to enforce the transverse momentum cut veto would be a necessary choice, however which may also suppress some useful signals.

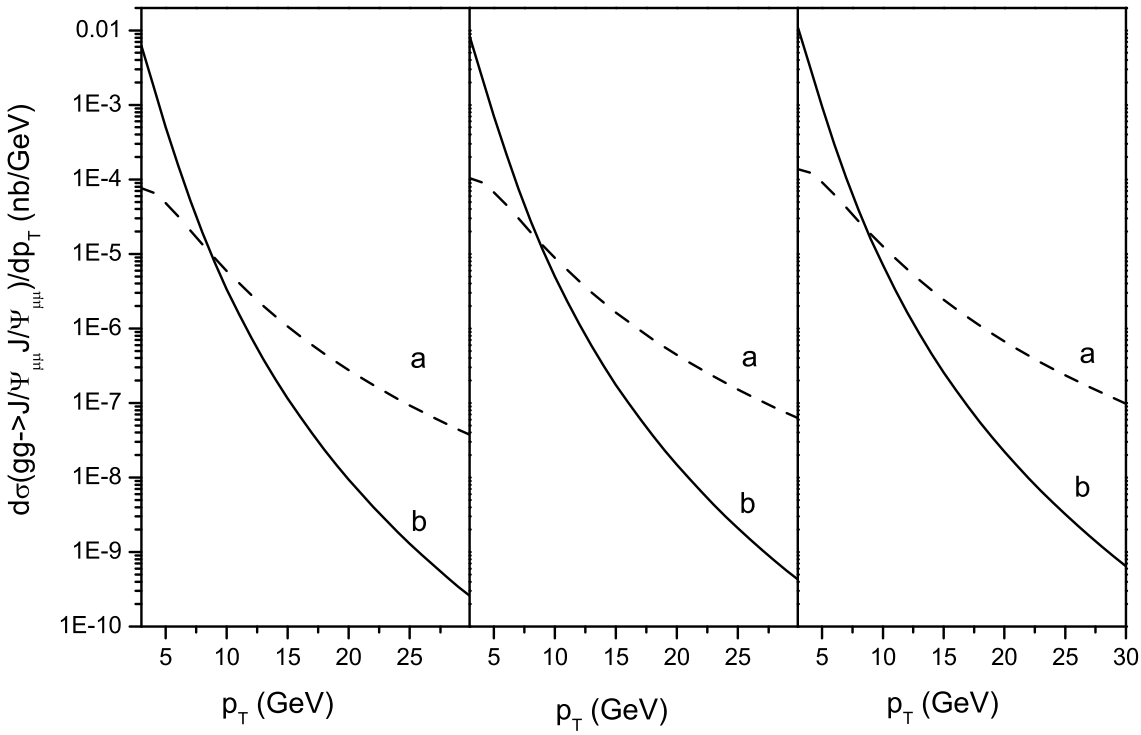

FIG. 5: The differential cross-section of J/ψ pair production versus p_T at the LHC. Lines a and b, represent yields from color-octet and color-singlet in unpolarized case, respectively. The diagrams from left to right represent for cases of $\sqrt{S} = 7$ TeV, $\sqrt{S} = 10$ TeV, and $\sqrt{S} = 14$ TeV, respectively.

The integrated cross sections of double J/ψ production with different polarizations are found to be measurable theoretically with a lower transverse momentum cut of 7 GeV in the first-year run of LHC at colliding energy of 7 TeV and luminosity of $1fb^{-1}$ or so, where about one hundred of di-muons from J/ψ decays will be produced and the total yields from CS and CO are comparable. For lower transverse momentum cut higher than 7 GeV, the double J/ψ yield may mainly come from the color-octet scheme, under the circumstance of employing the nowadays prevailing magnitude of color-octet matrix element. At colliding energy of 7 TeV, our calculation result shows that the data with at least one J/ψ in a pair being longitudinally polarized are nearly fifty percent of the total yield with transverse momentum integration lower cut of 5 GeV of produced J/ψ. Different from the inclusive production, where experimental data show that J/ψs tend to be unpolarized or

even longitudinally polarized with the increase of transverse momentum, in the exclusive pair production both color-singlet and -octet schemes exhibit that the produced J/ψ data should be always dominated by the transversely polarized yields. The above conclusions might be testified in future LHC experiment, and we expect the experiment measurement on exclusive double J/ψ production may tell us more on the charmonium production mechanism.

Acknowledgments

This work was supported in part by the National Natural Science Foundation of China(NSFC) under the grants 10935012, 10928510, 10821063 and 10775179, by the CAS Key Projects KJCX2-yw-N29 and H92A0200S2, and by the Scientific Research Fund of GUCAS.

Appendix

The polarized differential cross sections in color-singlet model. Here, the symbol $\|\|\|$ represents for the situation of both J/ψ being longitudinally polarized; $\|\perp$ for one J/ψ being longitudinally polarized and the other being transversely polarized, and $\perp\perp$ for both J/ψs being transversely polarized. In these expressions, s, t, u are normal Mandelstam variables at the parton level.

$$
\begin{aligned}
A_{ab}^{\mu\nu\rho\sigma} \;=\; & \frac{64\alpha_s^2\pi|R(0)|^2\delta_{ab}}{9m(m^2-u)^2(u+t-2m^2)^3}((m^2-t)(27m^6-(13t+59u)m^4+\\
& (-t^2+33ut+31u^2)m^2-18tu^2)g^{\mu\sigma}g^{\nu\rho}-(p_4^\mu((m^2-u)(3m^2-2t-u)p_4^\sigma m^2\\
& +(31m^6-2(15t+34u)m^4+(-2t^2+70ut+35u^2)m^2-36tu^2)p_3^\sigma)+2p_2^\mu((7m^2\\
& +t-8u)(m^2-u)p_3^\sigma m^2+(21m^6-(13t+47u)m^4+(-t^2+33ut+25u^2)m^2\\
& -18tu^2)p_4^\sigma))g^{\nu\rho}+(m^2-t)(m^2-u)(29m^4+(2t-13u)m^2-18tu)g^{\mu\rho}g^{\nu\sigma}\\
& -2(m^2-t)(m^2-u)(15m^4+(t-16u)m^2+9u(u-t))g^{\mu\nu}g^{\rho\sigma}-(p_2^\mu(2(28m^6\\
& +(6t-62u)m^4+(-19t^2+14ut+33u^2)m^2+18t(t-u)u)p_2^\nu-(45m^6+2(4t\\
& -67u)m^4+(-38t^2+68ut+87u^2)m^2+36t(t-2u)u)p_3^\nu)-(m^2-u)(11m^4\\
& +(4t+21u)m^2-36tu)p_4^\mu p_2^\nu)g^{\rho\sigma}+g^{\mu\sigma}(2p_2^\nu((7m^2+t-8u)(m^2-u)p_4^\rho m^2\\
& +(21m^6-(13t+47u)m^4+(-t^2+33ut+25u^2)m^2-18tu^2)p_3^\rho)-(45m^6\\
& -14(2t+7u)m^4+(-2t^2+68ut+51u^2)m^2-36tu^2)p_3^\nu(p_3^\rho+p_4^\rho))\\
& +g^{\nu\sigma}(2p_2^\mu((25m^2-17t-8u)(m^2-u)p_3^\rho m^2+(3m^6+(23t-11u)m^4+(-19t^2\\
& -21ut+7u^2)m^2+18t^2u)p_4^\rho)-(m^2-u)(11m^4+(4t+21u)m^2-36tu)p_4^\mu(p_3^\rho\\
& +p_4^\rho))-g^{\mu\rho}(2p_2^\nu((25m^2-17t-8u)(m^2-u)p_4^\sigma m^2+(3m^6+(23t-11u)m^4\\
& +(-19t^2-21ut+7u^2)m^2+18t^2u)p_3^\sigma)+p_3^\nu((5m^6+(32u-42t)m^4+(38t^2\\
& +2ut-35u^2)m^2+36tu(u-t))p_3^\sigma-(m^2-u)(39m^4-(38t+37u)m^2\\
& +36tu)p_4^\sigma))+g^{\mu\nu}(p_4^\rho(2(m^2-u)(16m^2-17t+u)p_4^\sigma m^2+(63m^6-2(14t\\
& +67u)m^4+(-38t^2+104ut+69u^2)m^2+36t(t-2u)u)p_3^\sigma)+(m^2-u)p_3^\rho(2(16m^2\\
& -17t+u)p_3^\sigma m^2+(-7m^4+(4t+39u)m^2-36tu)p_4^\sigma))-36(m^2-u)(p_2^\mu(2(m^2\\
& -t)p_2^\nu(p_3^\rho p_4^\sigma-p_4^\rho p_3^\sigma)+p_3^\nu(p_4^\rho((m^2-2t+u)p_3^\sigma+2(t-m^2)p_4^\sigma)-(m^2-2t+u)p_3^\rho p_4^\sigma))\\
& +p_4^\mu(p_3^\nu(p_3^\rho+p_4^\rho)((m^2-u)p_4^\sigma-(m^2-2t+u)p_3^\sigma)+p_2^\nu((m^2-u)p_4^\rho p_3^\sigma+p_3^\rho(2(m^2
\end{aligned}
$$

$$-t)p_3^\sigma + (u-m^2)p_4^\sigma))))) \tag{9}$$

Here, μ and ν are polarization indices of outgoing J/ψs, ρ and σ are polarization indices of initial gluons, a and b stand for colors.

$$M_{ab}^{\mu\nu\rho\sigma} = A_{ab}^{\mu\nu\rho\sigma} + A_{ab}^{\nu\mu\rho\sigma}(p_3 \leftrightarrow p_4, u \leftrightarrow t) \tag{10}$$

$$\frac{d\hat{\sigma}_{total}}{dt} = \frac{1}{8192\pi s^2}\sum_\lambda\sum_{ab}|(M\cdot\varepsilon(\lambda_{p_1})\varepsilon(\lambda_{p_2})\varepsilon(\lambda_{p_3})\varepsilon(\lambda_{p_4}))|^2 \tag{11}$$

$$\frac{d\hat{\sigma}_{\parallel\parallel}}{dt} = \frac{1}{8192\pi s^2}\sum_\lambda\sum_{ab}|(M\cdot\varepsilon(\lambda_{p_1})\varepsilon(\lambda_{p_2})\varepsilon(\lambda_{p_3})_{\parallel\parallel}\varepsilon(\lambda_{p_4})_{\parallel\parallel})|^2 \tag{12}$$

$$\begin{aligned}\frac{d\hat{\sigma}_{\parallel\perp}}{dt} = \frac{1}{8192\pi s^2}\sum_\lambda\sum_{ab}(&|(M\cdot\varepsilon(\lambda_{p_1})\varepsilon(\lambda_{p_2})\varepsilon(\lambda_{p_3})_{\parallel\parallel}\varepsilon(\lambda_{p_4})_{\perp\perp})|^2\\ &+|(M\cdot\varepsilon(\lambda_{p_1})\varepsilon(\lambda_{p_2})\varepsilon(\lambda_{p_3})_{\perp\perp}\varepsilon(\lambda_{p_4})_{\parallel\parallel})|^2)\end{aligned} \tag{13}$$

$$\frac{d\hat{\sigma}_{\perp\perp}}{dt} = \frac{1}{8192\pi s^2}\sum_\lambda\sum_{ab}|(M\cdot\varepsilon(\lambda_{p_1})\varepsilon(\lambda_{p_2})\varepsilon(\lambda_{p_3})_{\perp\perp}\varepsilon(\lambda_{p_4})_{\perp\perp})|^2 \tag{14}$$

$$\sum_\lambda\varepsilon(\lambda_{p_2})^\mu * \varepsilon(\lambda_{p_2})^\nu = \sum_\lambda\varepsilon(\lambda_{p_1})^\mu * \varepsilon(\lambda_{p_1})^\nu = -g^{\mu\nu} + \frac{p_1^\mu p_2^\nu + p_2^\mu p_1^\nu}{p_1\cdot p_2} \tag{15}$$

$$\sum_\lambda\varepsilon(\lambda_{p_3})^\mu * \varepsilon(\lambda_{p_3})^\nu = -g^{\mu\nu} + \frac{p_3^\mu p_3^\nu}{m^2} \tag{16}$$

$$\sum_\lambda\varepsilon(\lambda_{p_3})_{\perp\perp}^\mu * \varepsilon(\lambda_{p_3})_{\perp\perp}^\nu = -g^{\mu\nu} + \frac{p_3^\mu n_1^\nu + p_3^\nu n_1^\mu}{n_1\cdot p_3} - \frac{m^2 n_1^\mu n_1^\nu}{(n_1\cdot p_3)^2} \tag{17}$$

$$\sum_\lambda\varepsilon(\lambda_{p_3})_{\parallel\parallel}^\mu * \varepsilon(\lambda_{p_3})_{\parallel\parallel}^\nu = \frac{p_3^\mu p_3^\nu}{m^2} - \frac{p_3^\nu n_1^\mu + p_3^\mu n_1^\nu}{n_1\cdot p_3} + \frac{m^2 n_1^\mu n_1^\nu}{(n_1\cdot p_3)^2} \tag{18}$$

Here, $n_1 = (1, -\vec{p_3})$, $n_1^2 = 0$, and the polarized sum rule of $\varepsilon(\lambda_{p_4})$ is similar to that of $\varepsilon(\lambda_{p_3})$.

[1] G.T. Bodwin, E. Braaten, and G.P. Lepage, Phys. Rev. D**51**, 1125(1995).

[2] G.T. Bodwin, E. Braaten, and G.P. Lepage, Phys. Rev. D**46**, R3703(1992); E. Braaten and S. Fleming, Phys. Rev. Lett. **74**, 3327(1995).

[3] CDF Collaboration, F. Abe *et al.*, Phys. Rev. Lett. **69**, 3704(1992); **79**, 572(1997); **79**, 578(1997).

[4] E. Braaten, S. Fleming and A.K. Leibovich Phys. Rev. D**63**, 094006(2001).

[5] E. Braaten and J. Lee, Phys. Rev. D**67**, 054007(2003)[Erratum-ibid. D **72**, 099901 (2005)]; K.Y. Liu, Z.G. He and K.T. Chao, Phys. Lett. **B557**, 45(2003); K. Hagiwara, E. Kou, and C.-F. Qiao, Phys. Lett. **B570**, 39(2003).

[6] BELLE Collaboration, K. Abe, *et al.*, Phys. Rev. Lett. **89**, 142001(2002); *ibid*, Phys. Rev. D**70**, 071102(2004).

[7] BABAR Collaboration, B. Aubert, *et al.*, Phys. Rev. D**72**, 031101(2005).

[8] P. Cho and A.K. Leibovich, Phys. Rev. D**54**, 6690(1996); F. Yuan, C.-F. Qiao, and K.-T. Chao, Phys. Rev. D**56**, 321 (1997); *ibid*, 1663(1997); S. Baek, P. Ko, J. Lee, and H.S. Song, J. Korean, Phys. Soc. **33**, 97(1998); V.V. Kiselev, *et al.*, Phys. Lett. **B332**, 411(1994).

[9] BaBar Collaboration, B. Aubert, *et al.*, Phys. Rev. Lett. **87**, 162002(2001); Belle Collaboration, K. Abe, *et al.*, Phys. Rev. Lett. **88**, 052001(2002).

[10] Y.-J. Zhang, Y.-J. Gao and K.-T. Chao, Phys. Rev. Lett. **96**, 092001(2006); B. Gong and J. X. Wang, Phys. Rev. D**77**, 054028(2008).

[11] Yan-Qing Ma, Yu-Jie Zhang, Kuang-Ta Chao, e-Print: arXiv:0812.5106[hep-ph]; Bin Gong, Jian-Xiong Wang, e-Print: arXiv:0901.0117[hep-ph].

[12] Y.-J. Zhang, Y.-Q. Ma, and K.-T. Chao, Phys. Rev. D**78**, 054006(2008); G.T. Bodwin, D. Kang and J. Lee, Phys. Rev. D**74**, 014014(2006); G.T. Bodwin, D. Kang and J. Lee, Phys. Rev. D74, 114028(2006).

[13] P. Artoisenet, John M. Campbell, F. Maltoni, F. Tramontano, e-Print: arXiv:0901.4352[hep-ph]; Chao-Hsi Chang, Rong Li, Jian-Xiong Wang, e-Print: arXiv:0901.4749[hep-ph].

[14] John M. Campbell, F. Maltoni, F. Tramontano, Phys. Rev. Lett. **98**, 252002(2007); J.P. Lansberg and F. Maltoni, Phys. Lett. **B653**, 60(2007); Bin Gong and Jian-Xiong Wang, phys. Rev. Lett. **100**, 232001(2008); Bin Gong and Jian-Xiong Wang, Phys. Rev. **D78**, 074011(2008).

[15] Kaoru Hagiwara, W. Qi, C.-F. Qiao, and J.X. Wang, to appear in the Proceedings of the 34th International Conference on High Energy Physics, Philadelphia, 2008, [arXiv:0705.0803].

[16] J.P. Lansberg, Int. J. Mod. Phys. **A21**, 3857(2006).

[17] Quarkonium Working Group, N. Brambilla *et al*, CERN Yellow Report, e-Print: hep-ph/0412158.

[18] M. Kramer, Prog. Part. Nucl. Phys. **47**, 141(2001).

[19] P. Cho and M.B. Wise, Phys. Lett. **B346**, 129(1995).

[20] V. Barger, S. Fleming, and R.J.N. Phillips, Phys. Lett. **B371**, 111(1996).

[21] Cong-Feng Qiao, Phys. Rev. D**66**, 057504(2002).

[22] R. Mertig, M. Böhm, and A. Denner, Comput. Phys. Commun. **64**, 345(1991).

[23] CDF Collaboration, F. Abe *et al.*, Phys. Rev. Lett. **85**, 2886(2000).

[24] R.J. Cropp, FERMILAB-THESIS-2000-03.

[25] P. Cho and Leibovich, Phy. Rev. **D53**, 150(1996); *ibid*, 6203(1996).

[26] private communication with Guo-Min Chen.

[27] CTEQ Collaboration, H.L. Lai *et al.*, Eur. Phys. J. C**12**, 375(2000).